the plant journal

SEB SOCIETY FOR EXPERIMENTAL BIOLOGY

The Plant Journal (2009) **59**, 27–38 doi: 10.1111/j.1365-313X.2009.03844.x

Molecular and reverse genetic characterization of *NUCLEOSOME ASSEMBLY PROTEIN1* (*NAP1*) genes unravels their function in transcription and nucleotide excision repair in *Arabidopsis thaliana*

Ziqiang Liu[1,2], Yan Zhu[1], Juan Gao[1,2], Fang Yu[1,2,†], Aiwu Dong[1,*] and Wen-Hui Shen[2,*]

[1]*State Key Laboratory of Genetic Engineering, Department of Biochemistry, Institute of Plant Biology, School of Life Sciences, Fudan University, Shanghai 200433, PR China, and*

[2]*Institut de Biologie Moléculaire des Plantes (IBMP), Centre National de la Recherche Scientifique (CNRS), Université de Strasbourg (UdS), 12 rue du Général Zimmer, 67084 Strasbourg Cédex, France*

Received 11 December 2008; revised 4 February 2009; accepted 10 February 2009; published online 18 March 2009.

[*]For correspondence (fax +33 3 88 61 44 42; e-mail Wen-Hui.Shen@ibmp-ulp.u-strasbg.fr; fax +86 21 65643603; e-mail aiwudong@fudan.edu.cn).

[†]Present address: Department of Molecular Biology, Princeton University, Princeton, NJ 08544, USA.

SUMMARY

Compared with the well-studied biochemical function of NUCLEOSOME ASSEMBLY PROTEIN1 (NAP1) as a histone chaperone in nucleosome assembly/disassembly, the physiological roles of NAP1 remain largely uncharacterized. Here, we define the *NAP1* gene family members in Arabidopsis, examine their molecular properties, and use reverse genetics to characterize their biological roles. We show that the four AtNAP1-group proteins can form homodimers and heterodimers, can bind histone H2A, and are localized abundantly in the cytoplasm and weakly in the nucleus at steady state. AtNAP1;4 differs from the others by showing inhibitor-sensitive nucleocytoplasmic shuttling and tissue-specific expression, restricted to root segments and pollen grains. The other three *AtNAP1* genes are ubiquitously expressed in plants and the AtNAP1;3 protein is detected as the major isoform in seedlings. We show that disruption of the *AtNAP1*-group genes does not affect normal plant growth under our laboratory conditions. Interestingly, two allelic triple mutants, *Atnap1;1-1 Atnap1;2-1 Atnap1;3-1* and *Atnap1;1-1 Atnap1;2-1 Atnap1;3-2*, exhibit perturbed genome transcription, and show hypersensitivity to DNA damage caused by UV-C irradiation. We show that AtNAP1;3 binds chromatin, with enrichment at some genes involved in the nucleotide excision repair (NER) pathway, and that the expression of these genes is downregulated in the triple mutants. Taken together, our results highlight conserved and isoform-specific properties of AtNAP1 proteins, and unravel their function in the NER pathway of DNA damage repair.

Keywords: histone chaperone, chromatin, epigenetics, DNA repair, genotoxic stress, Arabidopsis.

INTRODUCTION

In plants, as in other eukaryotes, the basic structural unit of chromatin is the nucleosome. It consists of 146 base pairs (bp) of DNA wrapped around a histone octamer that contains two molecules each of H2A, H2B, H3 and H4 (Luger *et al.*, 1997). The octamer is structured by the H3/H4 tetramer at the center, and the two H2A/H2B dimers attached symmetrically on either side. The H3/H4 tetramer organizes the central portion of nucleosomal DNA, whereas each H2A/H2B dimer contacts about 30 bp on either side. Dynamic processes of nucleosome assembly, disassembly and reassembly occur during transcription, DNA replication, repair and recombination. Histone chaperones are involved in both the deposition of histones during nucleosome assembly and the eviction of histones during nucleosome disassembly. Histone chaperones are also thought to play roles in histone transfer to enzymes using histones as a substrate, in the storage of histone pools during development and in buffering transient histone overload (De Koning *et al.*, 2007).

NUCLEOSOME ASSEMBLY PROTEIN1 (NAP1) represents the primary chaperone of histones H2A and H2B, and is

highly conserved from yeast to humans (Park and Luger, 2006a). In *Saccharomyces cerevisiae*, NAP1 is encoded by a single gene, and a NAP1-deficient strain shows perturbed expression of about 10% of all nuclear genes, and a mild elongated-bud phenotype (Altman and Kellogg, 1997; Ohkuni *et al.*, 2003). In *Drosophila melanogaster*, the loss of NAP1 leads to embryonic lethality or weakly viable adults (Lankenau *et al.*, 2003). In mammals, NAP1 belongs to a multigene family (Park and Luger, 2006a), and the knock-out of the mouse neuron-specific *NAP1-homolog-2* gene is embryo lethal at the mid-gestation stage (Rogner *et al.*, 2000). Heterologous *NAP1* expression in slow-growing pulmonary artery endothelial cells increases their growth potential, whereas the inhibition of *NAP1* expression in fast-growing pulmonary microvascular endothelial cells decreases their growth potential (Clark *et al.*, 2008).

In plants, the first cDNA encoding NAP1 was reported in soybean (Yoon *et al.*, 1995). Later studies revealed that tobacco (*Nicotiana tabacum*), rice (*Oryza sativa*) and Arabidopsis (*Arabidopsis thaliana*) NAP1 proteins also belong to multigene families (Dong *et al.*, 2003, 2005). Whereas the fusion proteins GFP-Oryza;NAP1;1 and GFP-Oryza;NAP1;3 are localized in the cytoplasm and the nucleus, the GFP-Oryza;NAP1;2 and GFP-Nicta;NAP1;1–GFP-Nicta;NAP1;4 proteins are all primarily localized in the cytoplasm of transgenic tobacco BY2 cells (Dong *et al.*, 2003, 2005). Inhibitor treatment and mutation analysis revealed that the GFP-Oryza;NAP1;1 and GFP-Nicta;NAP1;1 proteins shuttle between the cytoplasm and the nucleus (Dong *et al.*, 2005). The Arabidopsis protein AtNAP1;1 is localized abundantly in the cytoplasm, but is also found in the nucleus at an early stage of leaf development (Galichet and Gruissem, 2006). Overexpression of *AtNAP1;1* slightly inhibits first-leaf growth, whereas the downregulation of *AtNAP1;1* slightly enhances first-leaf growth at an early stage after seed germination (Galichet and Gruissem, 2006). In contrast to the predominant cytoplasmic localization of NAP1 proteins, the Arabidopsis NAP1-related proteins NRP1 and NRP2 are primarily localized in the nucleus (Zhu *et al.*, 2006). Whereas the single *nrp1-1* and *nrp2-1* mutants have a wild-type phenotype, the double *nrp1-1 nrp2-1* mutant has a short-root phenotype and shows increased sensitivity to genotoxic stress (Zhu *et al.*, 2006). Like tobacco NAP1 proteins (Dong *et al.*, 2005), NRP1 and NRP2 preferentially bind histones H2A and H2B (Zhu *et al.*, 2006).

In addition to AtNAP1;1, NRP1 and NRP2, Arabidopsis plants contain three other genes encoding NAP1, namely *AtNAP1;2*, *AtNAP1;3* and *AtNAP1;4*. To provide a more comprehensive understanding of NAP1 function, we report here on the molecular, genetic and functional characterization of different *AtNAP1* genes. We show that all four AtNAP1 proteins have the capacity to form homodimers and heterodimers among them, but not with NRP1. All four AtNAP1 proteins are localized primarily in the cytoplasm, with at least AtNAP1;4 being able to shuttle between the cytoplasm and the nucleus. The *AtNAP1;4* gene is tissue-specifically expressed in root segments and pollen grains, which contrasts with the ubiquitous expression pattern of the other three *AtNAP1* genes. Western blot analysis revealed that AtNAP1;3 is the most abundant isoform of AtNAP1 proteins in young plants. Subcellular fractionation showed that most of AtNAP1;3 is present in the cytoplasm, with only a small fraction being found in the nucleus. To investigate the functions of the three ubiquitously expressed *AtNAP1* genes, we obtained loss-of-function mutants of these genes, as well as double and triple mutants. Under our laboratory standard growth conditions, all these mutants showed a wild-type phenotype. Transcriptome analysis revealed that 402 genes are downregulated and 86 genes are upregulated to more than twofold in both *Atnap1;1-1 Atnap1;2-1 Atnap1;3-1* and *Atnap1;1-1 Atnap1;2-1 Atnap1;3-2* triple mutants, compared with wild-type seedlings. Physiological phenotype tests revealed that the triple mutant seedlings have a decreased capacity of recovery after exposure to UV-C irradiation. Consistently, several genes involved in the nucleotide excision repair (NER) pathway, including *AtCEN1* (*At3g50360*), *AtCEN2* (*At4g37010*), *AtXPB* (*At5g41370* and *At5g41360*) and *AtXPC* (*At5g16630*) (Costa *et al.*, 2001; Molinier *et al.*, 2004; Kunz *et al.*, 2005; Morgante *et al.*, 2005; Liang *et al.*, 2006), are downregulated in the triple mutant seedlings, and a reduced efficiency of the *in vitro* repair of UV-induced DNA lesions was observed with protein extracts of the triple mutants, compared with wild-type plants. Chromatin immunoprecipitation (ChIP) analyses revealed that AtNAP1;3 binds chromatin with enrichment at *AtCEN1*, *AtCEN2* and *AtXPB*, compared with *ACTIN*. Taken together, our results provide important information on *AtNAP1* genes, and unravel an essential role for *AtNAP1* in the NER pathway.

RESULTS

AtNAP1 proteins can self-bind and bind between each other, but not with NRP1

AtNAP1;1, AtNAP1;2 and AtNAP1;3 share 74–83% identity with each other, and 41–43% identity with AtNAP1;4, but only share <23% identity with NRP1 and NRP2 (for sequence alignments, see Figure S1). The functional NAP1 exists as a stable dimer (Park and Luger, 2006b), and previous studies using pull-down assays revealed that the tobacco proteins Nicta;NAP1;3 and Nicta;NAP1;4 self-bind and bind between each other (Dong *et al.*, 2005). The Arabidopsis proteins NRP1 and NRP2 also self-bind and bind between each other (Zhu *et al.*, 2006). We first investigated direct protein–protein interactions among AtNAP1 proteins using the yeast two-hybrid assay. As shown in Figure 1(a), AtNAP1;1, AtNAP1;2 and AtNAP1;3 can self-bind and bind between each other. It is interesting to note that in spite of its more

diverged sequence, AtNAP1;4 shows a higher binding activity with AtNAP1;1, AtNAP1;2 and AtNAP1;3. As expected for controls, the transcriptional factors ASYMMETRIC LEAVES1 (AS1) and AS2 show a positive binding activity, as has been previously reported by Xu *et al.* (2003), and two empty vectors or combinations of one empty vector with one *AtNAP1*-expressing vector (excepting *AtNAP1;4*) do not show positive results. Because of its autoactivation when cloned in the pGBKT7 vector, the self-binding activity of AtNAP1;4 could not be examined in the yeast two-hybrid assay. We further investigated protein–protein interactions in pull-down assays. Total protein extracts from plants expressing YFP-AtNAP1;2, YFP-AtNAP1;3 or YFP-AtNAP1;4 were precipitated by beads coated with 6xHis-AtNAP1;1, 6xHis-AtNAP1;2, 6xHis-AtNAP1;3, 6xHis-AtNAP1;4 or 6xHis-NRP1. As shown in Figure 1(b), YFP-AtNAP1;2, YFP-AtNAP1;3 and YFP-AtNAP1;4 bind 6xHis-AtNAP1;1, 6xHis-AtNAP1;2, 6xHis-AtNAP1;3 and 6xHis-AtNAP1;4, but not 6xHis-NRP1. H2A-YFP was found to bind 6xHis-fused AtNAP1 proteins as well as NRP1 (Figure 1b). Taken together, these results indicate that different AtNAP1 isoforms can form homodimers and heterodimers, but not with NRP1.

AtNAP1 proteins are abundantly localized in the cytoplasm

We investigated the subcellular localization of AtNAP1 proteins in living cells by using YFP as a marker of visualization. YFP alone is small enough to diffuse across the nuclear envelope, and is localized in the cytoplasm and the nucleus of transgenic Arabidopsis and tobacco BY2 cells (not shown). YFP-AtNAP1;1, YFP-AtNAP1;2, YFP-AtNAP1;3 and YFP-AtNAP1;4 were all found to be localized primarily in the cytoplasm of transgenic Arabidopsis (Figure 2a–d) and BY2 cells (Figure 2e–h). Treatment with the nuclear export inhibitor leptomycin B (LMB) revealed that YFP-AtNAP1;4 (Figure 2i), but not the other AtNAP1 isoforms (data not shown), shuttles between the cytoplasm and the nucleus in transgenic tobacco BY2 cells.

AtNAP1;3 is the major isoform present in seedlings, and a small fraction of AtNAP1 proteins can be detected in the nucleus

In order to facilitate the analysis of endogenous AtNAP1 proteins, we searched for antibodies recognizing AtNAP1 proteins. The antibody produced earlier against Nicta;NAP1;4 (Dong *et al.*, 2005) recognized the recombinant proteins AtNAP1;1, AtNAP1;2 and AtNAP1;3 with similar affinities, but did not cross-react with AtNAP1;4, NRP1 or NRP2 (Figure 3a). Western blot analyses on total protein extracts of 9-day-old Arabidopsis seedlings revealed that AtNAP1;1, AtNAP1;2 and AtNAP1;3 are present at this growth stage (Figure 3b). Comparison of wild-type with mutants (see later for mutant descriptions) indicates that AtNAP1;3 migrates at a higher molecular-weight position, and is present at a much more abundant level in the wild-type extract compared with AtNAP1;1 and AtNAP1;2 (Figure 3b). Both reverse transcription-polymerase chain reaction (RT-PCR) (Zhu *et al.*, 2006) and northern analyses

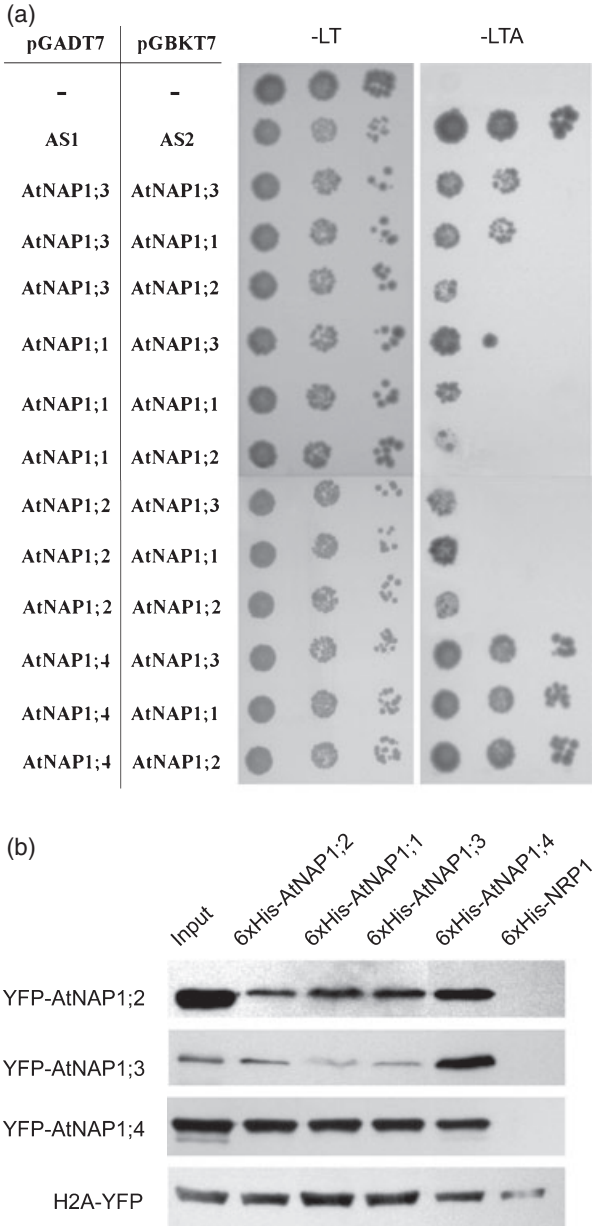

Figure 1. Protein–protein interactions.
(a) Yeast two-hybrid assay. Construct combinations of a pGADT7-based and a pGBKT7-based expression vector were co-transformed into the yeast strain AH109. A dilution (×10) series of yeast cells were plated onto media lacking leucine and tryptophan (–LT), or onto media lacking leucine, tryptophan and adenine (–LTA). The growth of yeast cells on –LTA plates indicates positive protein–protein interactions.
(b) Pull-down assay. Total protein extracts of transgenic Arabidopsis plants expressing YFP-AtNAP1;2, YFP-AtNAP1;3, YFP-AtNAP1;4 or H2A-YFP were incubated with beads coated with 6xHis-AtNAP1;1, 6xHis-AtNAP1;2, 6xHis-AtNAP1;3, 6xHis-AtNAP1;4 or 6xHis-NRP1, and the pull-down fractions were analyzed by Western blot using a polyclonal anti-GFP antibody (which cross-reacts with YFP). The input was loaded as the control.

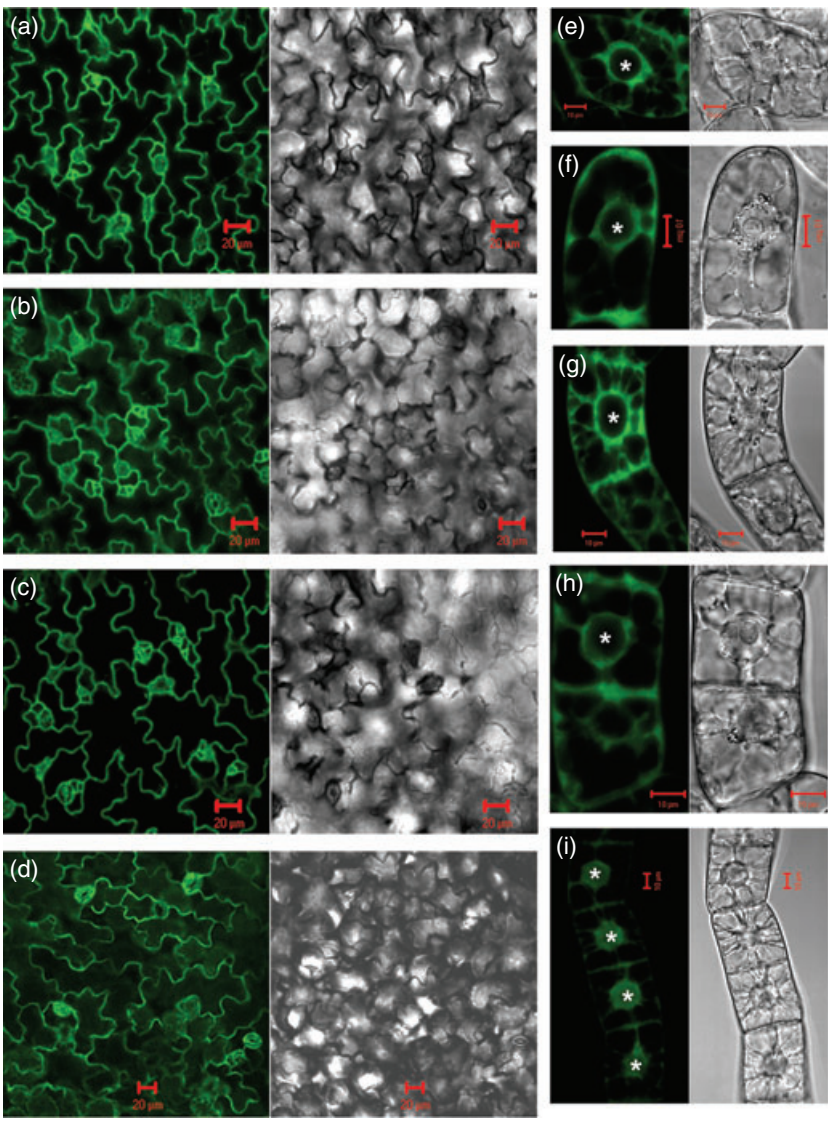

Figure 2. Subcellular localization of YFP-fused AtNAP1 proteins.
Leaf epidermal cells of transgenic Arabidopsis (a–d) and suspension cells of transgenic tobacco BY2 (e–i) expressing YFP-AtNAP1;1 (a, e), YFP-AtNAP1;2 (b, f), YFP-AtNAP1;3 (c, g) and YFP-AtNAP1;4 (d, h, i) were visualized by epifluorescence confocal microscopy. The YFP fluorescence (green) images are shown together with bright-field differential interference contrast images. The asterisks indicate the spherical nuclei. Note that the fluorescence is primarily found in the cytoplasm, except in panel (i), where YFP-AtNAP1;4 was found in the nucleus upon treatment with the nuclear export inhibitor leptomycin B (LMB). Scale bars: 20 μm (a–d); 10 μm (e–i).

(not shown) indicate that although the *AtNAP1;4* transcript level is barely detectable (see below for the specific expression of *AtNAP1;4*), the transcript levels of *AtNAP1;1*, *AtNAP1;2* and *AtNAP1;3* are similarly high. It is thus likely that a post-transcriptional mechanism differentially regulates the protein synthesis and/or stability of AtNAP1;3, compared with AtNAP1;1 and AtNAP1;2.

We further examined the cytoplasmic and nuclear distribution of AtNAP1 proteins by subcellular fractionation. As shown in Figure 3(c), the AtNAP1 proteins (mostly AtNAP1;3) are found in the total and cytoplasmic fractions, and are also found in the nuclear fraction, but at a much lower level. The controls, dimethyl-histone H4 lysine 4 (H3K4m2) as a nuclear marker and tubulin as a cytoplasmic marker, yield the expected results (Figure 3c), thereby validating our fractionation. These results are consistent with previous observations on the predominant cytoplasmic localization of AtNAP1 proteins, and provide additional information by showing that small quantities of AtNAP1 proteins are present in the nucleus. The detection of AtNAP1 proteins in the nucleus conforms their proposed histone chaperone activities in nucleosome assembly/disassembly.

AtNAP1;4 is tissue-specifically expressed in root segments and pollen grains

Previous RT-PCR analysis revealed that *AtNAP1;1*, *AtNAP1;2* and *AtNAP1;3* genes are ubiquitously expressed in all material examined, including seedlings, roots, stems and young flower buds, whereas the expression of *AtNAP1;4* was undetectable using up to 30 cycles of amplification (Zhu *et al.*, 2006). To test the possibility that *AtNAP1;4* is expressed in a low number of cells of specific types, we fused the β-glucuronidase (*GUS*) cDNA to the genomic clone of *AtNAP1;4* (Figure 4a). The clone contained the exons and

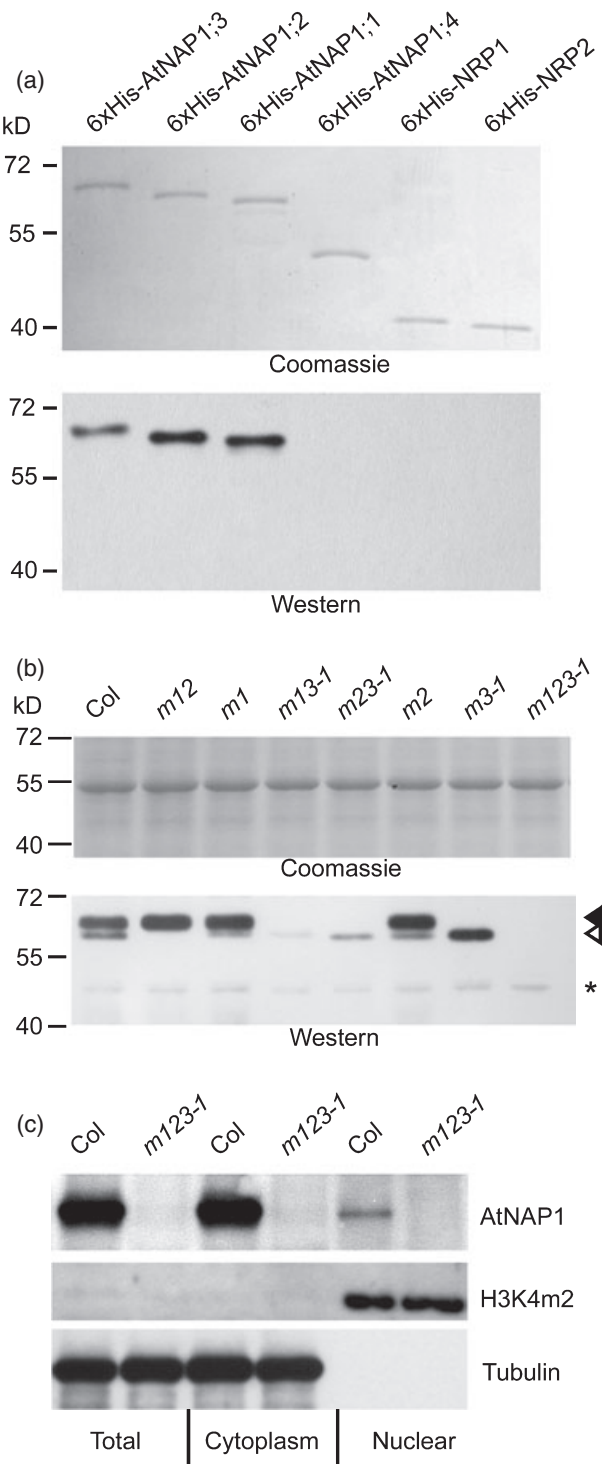

Figure 3. Western blot analyses of AtNAP1 proteins.
(a) Antibody quality test: 0.1-μg portions of recombinant proteins 6xHis-AtNAP1;1, 6xHis-AtNAP1;2, 6xHis-AtNAP1;3, 6xHis-AtNAP1;4, 6xHis-NRP1 and 6xHis-NRP2 were analyzed. The upper panel shows Coomassie staining of the gel, and the lower panel shows Western blot results using the antibody initially raised against Nicta;NAP1;4. Note that the antibody cross-reacts with AtNAP1;1, AtNAP1;2 and AtNAP1;3, but not with AtNAP1;4, NRP1 and NRP2.
(b) Detection of AtNAP1 proteins in wild-type (Col) and mutant plants. A total of 10 μg of total protein extracts from 9-day-old seedlings were analyzed using the same antibody as described in (a): the solid arrowhead indicates the position of AtNAP1;3; the open arrowhead indicates the position of AtNAP1;1 and AtNAP1;2, which migrate closely together; and the asterisk indicates an unknown protein that shows a weak unspecific signal that is found in all samples.
(c) Subcellular fractionation of 9-day-old wild-type (Col) and the *m123-1* mutant seedlings: 10 μg of total proteins and the corresponding equivalent cytoplasmic and nuclear fractions were analyzed. AtNAP1 was detected using the antibody described above. H3K4m2, specifically present in the nucleus, and tubulin, specifically present in the cytoplasm, serve as fractionation quality controls.

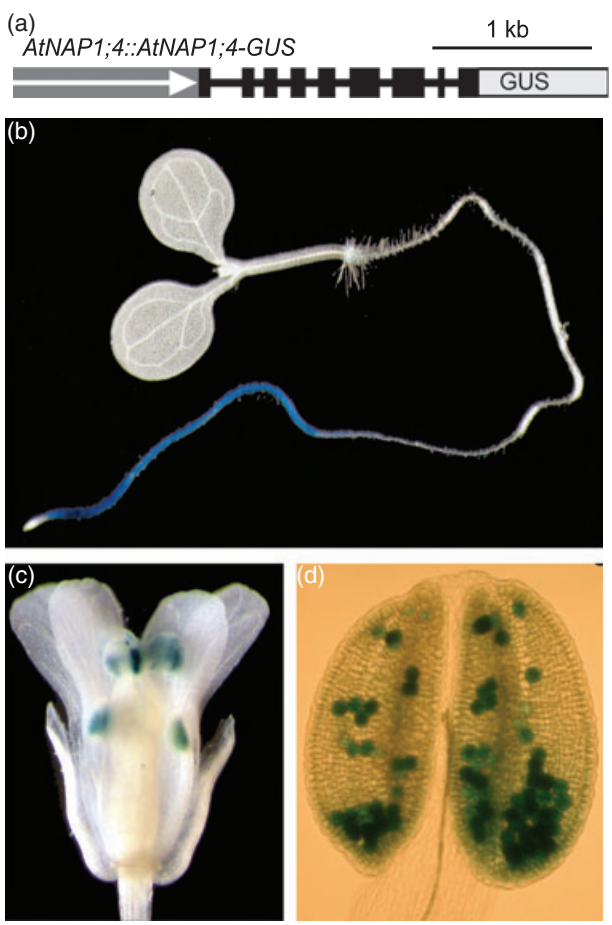

Figure 4. Tissue-specific expression of *AtNAP1;4*.
(a) Gene structures of *AtNAP1;4::AtNAP1;4-GUS*. The gray box with white arrow represents the promoter, dark boxes represent exons, lines represent introns, and the last exon is fused in frame with the reporter GUS, as indicated.
(b–d) Histochemical analysis of *AtNAP1;4::AtNAP1;4-GUS* expression in a 5-day-old seedling (b), in a flower (c) and in an anther (d).

introns, as well as 619 bp of the upstream sequences from the predicted translational start site of the *AtNAP1;4* gene. Consistent with the RT-PCR study, *AtNAP1;4::AtNAP1;4-GUS* activity was undetectable in most plant tissues examined, except the root segment covering the apical end of the differentiation zone, the elongation zone of the root (Figure 4b) and the mature pollen within the anthers of open

flowers (Figure 4c,d). This tissue-specific expression of *AtNAP1;4::AtNAP1;4-GUS* was reproducibly observed in eight independent transgenic lines. Re-examination by RT-PCR revealed that *AtNAP1;4* transcripts were detectable from wild-type inflorescences using 41 cycles of amplification (data not shown).

Production and characterization of the loss-of-function of *Atnap1* mutants

To investigate the function of AtNAP1, we obtained T-DNA insertion lines from the Arabidopsis Biological Resource Center (ABRC, http://www.biosci.ohio-state.edu/~plantbio/Facilities/abrc/abrchome.htm). One T-DNA insertion mutant allele each was identified for *AtNAP1;1*, *AtNAP1;2* and *AtNAP1;4*, and two independent mutant alleles were identified for *AtNAP1;3* (Figure 5a). In all of these insertion lines, the T-DNA segregated as a single locus. Homozygous (hereafter called mutant) plants were obtained for each of these T-DNA insertion lines by self-pollination. For convenience, the mutants *Atnap1;1-1*, *Atnap1;2-1*, *Atnap1;3-1*, *Atnap1;3-2* and *Atnap1;4* were named *m1*, *m2*, *m3-1*, *m3-2* and *m4*, respectively. RT-PCR analysis revealed that the full-length transcripts of the corresponding genes were undetectable in the mutant plants (Figure 5b), indicating that T-DNA insertions caused the loss of function of the *AtNAP1* genes. None of the mutants showed detectable growth modifications. The increased growth of leaves previously reported for *Atnap1;1-1* (Galichet and Gruissem, 2006) was not reproduced under our *in vitro* culture and glasshouse growth conditions.

Considering their overlapping expression pattern and their high conservation of protein sequences and properties, it is likely that *AtNAP1* genes have redundant functions. Because *AtNAP1;4* differs from the other three *AtNAP1* genes and shows a tissue-specific expression, we subsequently focused our work on *m1*, *m2*, *m3-1* and *m3-2* to obtain double and triple mutants to investigate overlapping functions. Through crosses between different mutants, selfing segregation and PCR genotyping (see Figure S2), we obtained the double mutants *Atnap1;1-1 Atnap1;2-1* (*m12*), *Atnap1;1-1 Atnap1;3-1* (*m13-1*), *Atnap1;1-1 Atnap1;3-2* (*m13-2*), *Atnap1;2-1 Atnap1;3-1* (*m23-1*) and *Atnap1;2-1 Atnap1;3-2* (*m23-2*), as well as the triple mutants *Atnap1;1-1 Atnap1;2-1 Atnap1;3-1* (*m123-1*) and *Atnap1;1-1 Atnap1;2-1 tnap1;3-2* (*m123-2*). Remarkably, all these double and triple mutants show a wild-type phenotype (Figure 5c for *m123-1*; data not shown for other mutants). RT-PCR analyses confirmed that the corresponding *AtNAP1* genes were knocked down in the mutants (Figure 5b). Western blot analysis also confirmed that the corresponding AtNAP1 proteins were undetectable in the mutants (Figure 3b). In addition, we noticed that AtNAP1;3 levels were elevated in *m1*, *m2* and *m12*, and that AtNAP1;1/AtNAP1;2 levels were elevated in *m3-1* compared with wild-type seedlings (Figure 3b), suggesting a homeostatic compensation mechanism. Nonetheless, *AtNAP1;4* transcripts were undetectable in the seedlings of all mutants (including *m123-1* and *m123-2*) and the wild-type by RT-PCR, using up to 41 cycles of amplification. This last observation did not support the assumption that *AtNAP1;4* could be ectopically expressed, which would compensate for the loss of function of other AtNAP1 proteins in the mutants.

Perturbation of gene expression in *Atnap1* mutants

Plants with loss-of-function of *AtNAP1* genes grow in a macroscopically similar manner to wild-type plants under our laboratory *in vitro* culture and glasshouse growth

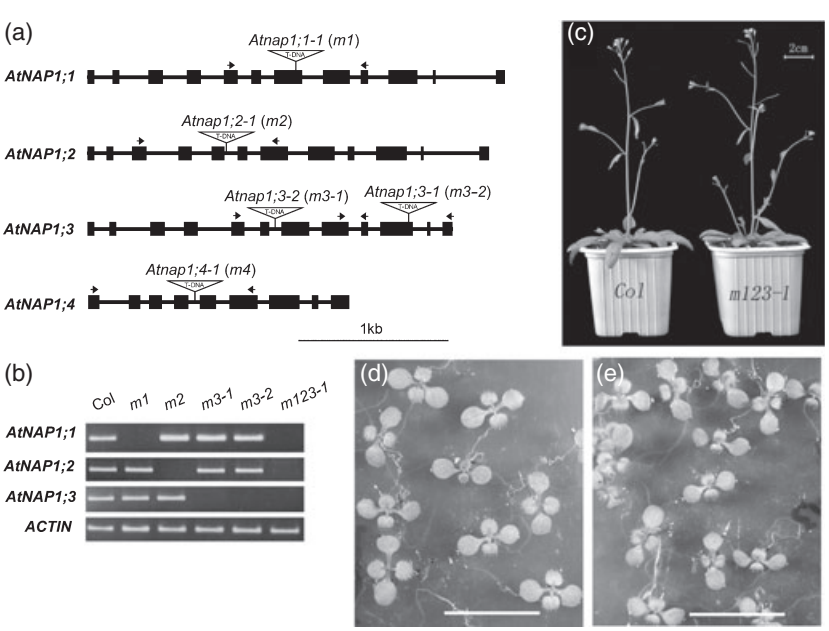

Figure 5. Loss-of-function mutants of *AtNAP1* genes.
(a) Gene structures of *Atnap1;1-1*, *Atnap1;2-1*, *Atnap1;3-1*, *Atnap1;3-2* and *Atnap1;4-1* mutant alleles. Dark boxes represent exons, lines represent introns, triangles indicate T-DNA insertions, and arrowheads indicate the positions of the PCR primers used in the genotyping of the mutants and gene expression analysis.
(b) RT-PCR analysis of expression of *AtNAP1;1*, *AtNAP1;2* and *AtNAP1;3* in wild-type (Col) and mutants plants. *ACTIN* (*AtACT7*) serves as an internal control.
(c) Comparison of a 28-day-old wild-type (Col) plant and the triple mutant *Atnap1;1-1 Atnap1;2-1 Atnap1;3-1* (*m123-1*).
(d, e) Comparison of 9-day-old seedlings of wild-type (d) and the triple mutant *m123-1* (e). Scale bars: 1 cm.

conditions. This is unexpected in view of the predicted fundamental function of NAP1 in nucleosome assembly. To investigate the molecular phenotypes of the mutant plants, we performed global transcriptome analysis. To avoid the redundancy problem of different *AtNAP1* genes, we focused on triple mutant analysis using the Affymetrix ATH1 array, which contains more than 22 500 probe sets, representing approximately 24 000 Arabidopsis genes (http://www.affymetrix.com/products/arrays/specific/arab.affx). In 6-day-old seedlings, 402 genes were found to be downregulated and 86 genes were found upregulated in both *m123-1* and *m123-2* mutants, compared with the wild type (Figure 6a). As expected, *AtNAP1;1*, *AtNAP1;2* and *AtNAP1;3* were among the downregulated genes. Among the differentially expressed genes found in triple mutants, some are potentially involved in protein phosphorylation, gene transcription, phytohormone and stress responses, and DNA repair (Table S1). We further investigated the expression of some DNA repair genes by quantitative RT-PCR analysis. Consistent with transcriptome data, we found that the expression of *AtCEN1*, *AtCEN2* and *AtXPB*, genes involved in the NER pathway (Costa *et al.*, 2001; Molinier *et al.*, 2004; Morgante *et al.*, 2005; Liang *et al.*, 2006), is downregulated by more than twofold in the *m123-1* mutant compared with the wild type (Figure 6b). The NER pathway gene *AtXPC* (Kunz *et al.*, 2005) was among the downregulated genes found in the *m123-2* mutant, but not in the *m123-1* mutant (Table S1). RT-PCR confirmed the downregulation of *AtXPC* in the *m123-2* mutant (not shown), and also revealed a downregulation of about 1.5-fold in the *m123-1* mutant (Figure 6b). In contrast, the other genes examined, including *AtXPD*, *AtXPF*, *AtXPG* and *AtRAD23-1*, which are potentially involved in the NER pathway (Kunz *et al.*, 2005), as well as *AtRAD51*, *AtRAD54* and *AtATM*, which are involved in the double-strand break (DSB) DNA repair pathway (Garcia *et al.*, 2003; Li *et al.*, 2004; Osakabe *et al.*, 2006), did not show major changes of expression in the mutant (Figure 6b). This is also consistent with transcriptome data. Analysis of gene expression in response to UV treatment revealed that expression of *AtCEN1*, *AtCEN2* and to a lesser degree *AtXPB* is induced by UV in both the wild type and the *m123-1* mutant, albeit at a weaker level in the mutant (Figure 6c). It indicates that AtNAP1 proteins are dispensable for initiation, but have an expression enhancer role for these genes.

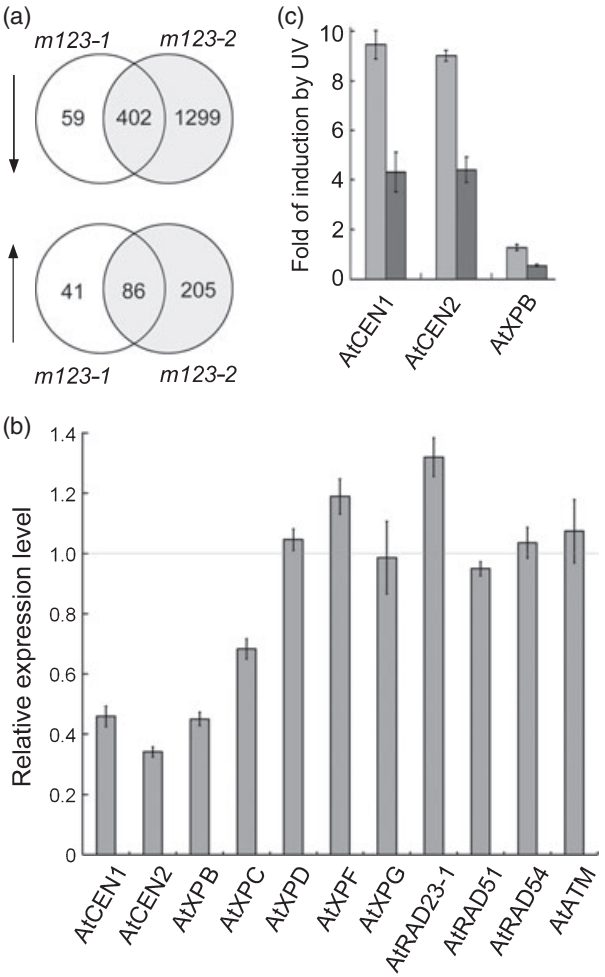

Figure 6. The perturbed expression of genes in the triple *AtNAP1* mutants.
(a) The Venn diagrams show the number and overlap of differentially expressed genes found in the triple gene mutants *Atnap1;1-1 Atnap1;2-1 Atnap1;3-1* (*m123-1*) and *Atnap1;1-1 Atnap1;2-1 Atnap1;3-2* (*m123-2*). Microarray analyses were performed using 6-day-old seedlings on the ATH1 Affymetrix gene chips, which cover 24 000 Arabidopsis genes. The arrows indicate the upregulated and downregulated categories of differentially expressed genes.
(b) Quantitative RT-PCR analysis of the expression of genes involved in DNA repair. The RT-PCR analyses were performed in two independent experiments. The mean values of the relative expression levels of genes in the *m123-1* mutant compared with wild-type plants are shown by columns, and the standard deviations are indicated by the error bars.
(c) Effects of UV-C irradiation on the expression of some genes involved in the nucleotide excision repair (NER) pathway. The -fold of induction was calculated from changes in expression levels after/before irradiation. Mean values are shown by the gray columns for wild-type plants and dark columns for *m123-1* plants, and the standard deviations are indicated by the error bars; data from three quantitative PCR repeats.

Atnap1 triple mutants show defects in UV-damage repair

The downregulation of some genes involved in the NER pathway prompted us to investigate the physiological phenotype of *Atnap1* triple mutants in response to DNA damages. We tested plant growth in the presence of bleomycin and hydroxyurea, inhibitors of the DSB repair pathway and DNA synthesis, respectively. No significant difference was observed between *m123-1* and wild-type plants in response to these inhibitors (data not shown). Interestingly, compared with the wild type, both *m123-1* and *m123-2* triple mutants exhibit a more pronounced reduction in growth and pale-green phenotype in response to UV-C damage (Figure 7a). The recovery rates of *m123-1* and *m123-2* were much lower than that of the wild type after UV-C treatment (Figure 7b).

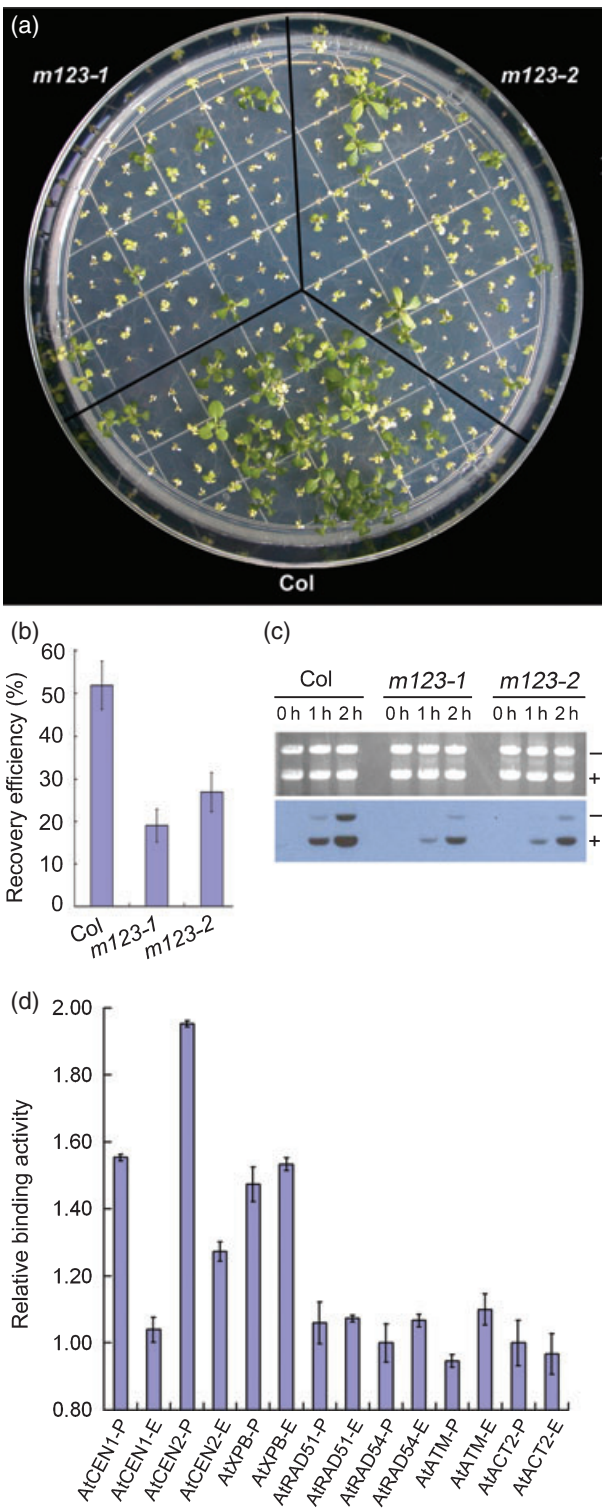

Figure 7. Analyses of the UV-C response of the triple *AtNAP1*-gene mutants compared with wild-type plants.
(a) Photograph of a plate showing plant growth 13 days after UV-C treatments. The wild-type (Col) and the triple mutants *Atnap1;1-1 Atnap1;2-1 Atnap1;3-1* (*m123-1*) and *Atnap1;1-1 Atnap1;2-1 Atnap1;3-2* (*m123-2*) were tested by growth on the same plate.
(b) Recovery efficiency of plant growth of wild-type (Col) and the mutants *m123-1* and *m123-2* 13 days after UV-C treatments. Columns represent mean values from two independent experiments, and the error bars represent standard deviations. A total of 160–200 plants were tested for each genotype.
(c) *In vitro* DNA repair assay of a UV-C-damaged plasmid. Protein extracts from wild-type (Col) and the *m123-1* and *m123-2* mutant plants were incubated with UV-C-damaged pBKS plasmid (+) and untreated pGEX plasmid (–) in the presence of DIG-labeled dUTP. The upper panel shows DNA staining and lower panel shows dUTP incorporation over a time course of up to 2 h.
(d) Chromatin immunoprecipitation (ChIP) assay for the relative chromatin-binding activity of AtNAP1;3 at the promoter (-P) and coding (-E) regions of DNA-repair genes, compared with *ACTIN* (*AtACT2*) as a control. Columns represent mean values from two independent experiments, and the error bars represent standard deviations.

We further investigated the efficiency of DNA repair by cell extracts of wild-type, *m123-1* and *m123-2* mutant plants using a previously described *in vitro* assay (Li *et al.*, 2002). In this assay, the DNA repair efficiency is evaluated by incorporation of DIG-labeled dUTP in a UV-damaged plasmid DNA. As shown in Figure 7c, cell extracts prepared from the mutant plants show a less efficient DNA repair efficiency than that from the wild-type plants (Figure 7c). Taken together, our data indicate that *AtNAP1* genes play important roles in the NER pathway, which is involved in the repair of DNA lesions caused by UV-C.

Using ChIP assays, we investigated the chromatin-binding activity of AtNAP1;3 at DNA repair genes. ChIP fractions from the *m12* and *m123-1* mutant plants were analyzed by quantitative PCR using gene-specific primers (see Table S2 for primer information). The values were normalized by input so as to minimize the variation introduced by the variable efficiency of the primers, then the values obtained in *m12* (in which AtNAP1;3 is present) were subtracted from those obtained in *m123-2* (in which AtNAP1;3 is absent) so as to enhance the specificity of detection of AtNAP1;3, and finally the relative binding activity at different regions within the promoters (*P*) and exons (*E*) of the genes were referenced against that at *AtACT2-P*, which is given a value of 1 (Figure 7d). The binding activity of AtNAP1;3 at *AtCEN1-E*, *AtRAD51*, *AtRAD54* and *AtATM* was found to be similar to that at *AtACT2*, whereas the binding activities at *AtCEN1-P*, *AtCEN2* and *AtXPB1* were about 1.3–1.9-fold higher. This higher binding activity correlates with the downregulation of *AtCEN1*, *AtCEN2* and *AtXPB1* found in the triple mutants *m123-1* and *m123-2*, thus suggesting that AtNAP1 proteins are positive regulators of expression of these NER-pathway genes.

DISCUSSION

Arabidopsis has four *NAP1*-group genes and two *NRP* genes. Although AtNAP1 and NRP proteins can all interact with H2A/H2B, our study reveals differences between the AtNAP1 and NRP groups of proteins at molecular, cellular and functional levels. NRP1 and NRP2 were previously reported to form homodimeric and heterodimeric com-

plexes (Zhu *et al.*, 2006). Here, we show that the four AtNAP1 proteins can form homodimeric and heterodimeric complexes, but they cannot bind NRP1, suggesting that the AtNAP1 and NRP proteins form group-specific complexes. Whereas YFP-fused proteins of NRP1 and NRP2 are localized in the nucleus (Zhu *et al.*, 2006), YFP-fused AtNAP1 proteins are primarily localized in the cytoplasm. YFP-AtNAP1;4 can shuttle between the nucleus and the cytoplasm, and a small fraction of AtNAP1;3 was found in the nuclear fraction. It appears that mechanisms exist to avoid overload of AtNAP1 proteins in the nucleus: an overload might interfere with nucleosome dynamics, causing genome dysfunction. Whereas *AtNAP1;4* shows specific expression in pollen and root segments, the other three *AtNAP1* genes are abundantly expressed in all plant organs examined. Furthermore, post-transcriptional mechanism(s) differentially regulate the product levels of the latter genes in such a way that AtNAP1;3 becomes the major isoform of AtNAP1 proteins. Finally, an analysis of *Atnap1* mutant plants revealed the compensatory homeostatic regulation of AtNAP1 protein levels. Together, these observations support the idea that the nature of the multigene family provides AtNAP1 with more flexibility to cope with the developmental and growth adaptation requirements of plants.

Although the functional redundancy of different *AtNAP1* genes could explain the wild-type phenotype of single and double mutants, before our study the triple mutants, *m123-1* and *m123-2*, were not predicted to exhibit a normal growth phenotype. Our findings indicate that AtNAP1 is dispensable for plant growth, and suggests that in the absence of AtNAP1, H2A/H2B might be chaperoned by other type(s) of factor(s). The first candidates for such factors are NRP1 and NRP2, which were previously characterized as H2A/H2B chaperones (Zhu *et al.*, 2006). Otherwise, FACILITATES CHROMATIN TRANSCRIPTION (FACT) and NUCLEOLIN could also fulfill H2A/H2B chaperone activities in Arabidopsis. Similar to those in AtNAP1 and NRPs, long acidic stretches are found in the Spt16 subunit of FACT (Duroux *et al.*, 2004) and in NUCLEOLIN (Kojima *et al.*, 2007; Petricka and Nelson, 2007; Pontvianne *et al.*, 2007). The human FACT possesses intrinsic histone H2A/H2B chaperone activity, which depends on the acidic region of Spt16 (Belotserkovskaya *et al.*, 2003). It has been shown that the acidic region of human NUCLEOLIN is required for its chaperone activity of H2A/H2B (Angelov *et al.*, 2006). Furthermore, the chromatin-binding properties of the Arabidopsis FACT (Duroux *et al.*, 2004) and chromatin disorganization observed in the *Atnuc-L1* mutant (Pontvianne *et al.*, 2007) are consistent with the proposed histone chaperone activity of FACT and NUCLEOLIN. We hypothesize that these distinct types of H2A/H2B chaperones (AtNAP1, NRPs, FACT and NUCLEOLIN) could be used to selectively modulate the dynamics of specific chromatin domains, and to provide overlapping functions to safeguard genome activity.

In spite of their normal growth phenotype, *m123-1* and *m123-2* mutants show perturbed gene expression. The perturbed genes include some genes that are potentially involved in DNA damage repair, protein phosphorylation/dephosphorylation and hormone responses (see Table S1), which suggests substantial roles for AtNAP1 in physiological processes. In this study, we focused on DNA damage repair, and showed that AtNAP1 is involved in the NER pathway.

The NER pathway is crucial, and contributes to global genome repair to eliminate most DNA lesions, particularly photochemical lesions such as the cyclobutane pyrimidine dimer and the pyrimidine (6–4) pyrimidine dimer (Sancar, 1996). In our study, cell extracts prepared from *m123-1* and *m123-2* mutant plants show less efficiency in the repair of UV-induced DNA lesions, compared with extracts from wild-type plants. In addition, both mutants showed lower recovery rates of plant growth after UV-C damage, compared with the wild type. Several genes involved in the NER pathway, including *AtCEN1*, *AtCEN2*, *AtXPB* and *AtXPC*, were found to be downregulated in both *m123-1* and *m123-2* mutants. AtCEN1 and AtCEN2 proteins are 65% identical, and both belong to the CENTRIN family of EF-hand calcium binding proteins. They are involved in microtubule organization and DNA repair (Molinier *et al.*, 2004; Liang *et al.*, 2006; Azimzadeh *et al.*, 2008). The human CENTRIN2 (HsCEN2) is considered to act at the initial step in the recognition of DNA lesions, and the human XPC–XPB complex acts at a second step as a helicase in unwinding the DNA encompassing the lesion (Kunz *et al.*, 2005). AtCEN2 is highly similar to HsCEN2 in sequence and in domain organization (Molinier *et al.*, 2004), and forms a protein complex in Arabidopsis similar to that in humans (Liang *et al.*, 2006). Arabidopsis harbors a duplication of the *XPB* ortholog, *AtXPB1* and *AtXPB2*, and the proteins encoded by the duplicated genes show 95% amino acid identity (Costa *et al.*, 2001; Morgante *et al.*, 2005). Our gene expression analysis covers both *AtXPB1* and *AtXPB2*. Consistent with functioning in the NER pathway, the AtCEN2 protein was shown to act in DNA repair both *in vitro* and *in vivo* (Molinier *et al.*, 2004; Liang *et al.*, 2006), and the knock-down of either *AtCEN2* (Molinier *et al.*, 2004) or *AtXPB1* (Costa *et al.*, 2001) resulted in an increased sensitivity of plants to DNA damage. Our data corroborate the previous studies on the role of AtCEN2 and AtXPB in DNA repair, and suggest that the downregulation of these NER-pathway genes caused the UV-sensitive mutant phenotypes in *m123-1* and *m123-2*. AtNAP1;3 binds chromatin with enrichment at *AtXPB*, *AtCEN1* and *AtCEN2*, indicating that AtNAP1 proteins may function as transcriptional activators of these NER-pathway genes. Histone chaperones could also be directly involved in the displacement or exchange of histones occurring during the process of NER (Dinant *et al.*, 2008). Such a role for NAP1-family proteins is, however, currently unknown.

In conclusion, we have shown that the four AtNAP1-group proteins have both conserved as well as isoform-specific properties. Our reverse-genetic approach unequivocally showed that AtNAP1-deficient plants can grow normally under laboratory conditions, but become hypersensitive to DNA damage caused by UV irradiation. We propose that AtNAP1 may function as a modulator of genome transcription in plant responses to environmental stress.

EXPERIMENTAL PROCEDURES

Plant materials and growth conditions

All *A. thaliana* alleles were derived from the Columbia ecotype. *Atnap1;1-1*, *Atnap1;2-1*, *Atnap1;3-1*, *Atnap1;3-2* and *Atnap1;4-1* alleles correspond to SALK_013610, SALK_131746, SAIL_373_H11, SAIL_84_B01 and BX290796 of T-DNA insertion lines from the ABRC. Different combinations of double and triple mutants were obtained in our laboratory by genetic crossing (see Figure S1). *In vitro* plant culture was performed on agar-solidified MS medium M0255 (Duchefa, http://www.duchefa.com), supplemented with 0.9% sucrose. Plants were grown at 21°C under 16-h light/8-h dark conditions.

Yeast two-hybrid assays

The *AtNAP1;1*, *AtNAP1;2*, *AtNAP1;3* and *AtNAP1;4* cDNAs were obtained by RT-PCR using primer pairs N123P1/N1P2, N123P1/N2P2, N123P1/N3P2 and N4P1/N4P2 (Table S2), respectively. The resulting PCR products were cloned in pGEM-T vector and then sequenced to confirm the absence of sequence errors, resulting in pGEM-T-AtNAP1;1, pGEM-T-AtNAP1;2, pGEM-T-AtNAP1;3 and pGEM-T-AtNAP1;4. The *AtNAP1* cDNAs were then subcloned into the pGBKT7 and pGADT7 vectors (Clontech, http://www.clontech.com). Constructs of AS1 and AS2 were described previously (Xu *et al.*, 2003). Protein–protein interactions were examined according to the manufacturer's recommendations (Clontech).

YFP-fusion vector construction and plant transformation

The *AtNAP1* cDNAs were cut from the pGEM-T vector, fused with the 3′ end of *YFP* cDNA and then subcloned under the control of the cauliflower mosaic virus (CaMV) 35S promoter in the pCAMBIA1301 binary vector (CAMBIA, http://www.cambia.org). The resulting plasmids were introduced into *Agrobacterium tumefaciens*, and the resulting strains were used to transform Arabidopsis plants and tobacco BY2 cells, as described previously (Yu *et al.*, 2003). Arabidopsis plants expressing H2A-YFP were also described previously (Yu *et al.*, 2003).

Production of recombinant proteins

The *AtNAP1* cDNAs were cut from the pGEM-T vector and subcloned into the pET-30a vector (Novagen, http://www.emdbiosciences.com/html/NVG/home.html) to produce 6xHis-tagged recombinant proteins. Vectors for 6xHis-NRP1 and 6xHis-NRP2 were previously described by Zhu *et al.* (2006). The production and purification of 6xHis-tagged recombinant proteins were performed as described by Dong *et al.* (2005).

Pull-down assays

A 10-mg portion of purified recombinant 6xHis-AtNAP1;1, 6xHis-AtNAP1;2, 6xHis-AtNAP1;3, 6xHis-AtNAP1;4 or 6xHis-NRP1 protein was coupled to 1 ml of BrCN-activated Sepharose 4B resin (Amersham, now part of GE Healthcare, http://www.gehealthcare.com). The resulting resin was used in the pull-down assays, according to a previously described protocol (Dong *et al.*, 2005). Total protein extracts from about 10 g of 2-week-old transgenic Arabidopsis plants expressing YFP-AtNAP1;2, YFP-AtNAP1;3, YFP-AtNAP1;4 or H2A-YFP were each distributed equally to the aforementioned five recombinant protein-coated resins. A quarter of each pull-down fraction was used for Western blot analysis.

Western blot

Proteins were separated by SDS–PAGE, and transferred to an Immobilon-P polyvinylidene difluoride transfer membrane (Millipore, http://www.millipore.com). The membrane was blotted with specific antibodies. The antibodies used in this study are: the anti-GFP rabbit polyclonal antibody (Molecular Probes, now part of Invitrogen, http://www.invitrogen.com/site/us/en/home/brands/Molecular-Probes.html) at a dilution of 1:5000, the anti-Nicta; NAP1;4 mice polyclonal antibodies (Dong *et al.*, 2005) at a dilution of 1:2000, the anti-dimethyl H3K4 (cat. no. 07-030; Millipore) at a dilution of 1:2000, the anti-α-tubulin monoclonal antibody (cat. no. T6199; Sigma-Aldrich, http://www.sigmaaldrich.com) at a dilution of 1:10 000.

Microscopy

The epifluorescence and differential interference contrast images were taken using a confocal laser scanning microscope (model LSM510; Zeiss, http://www.zeiss.com).

Subcellular protein fractionation

For subcellular fractionation, about 2 g of 9-day-old seedlings were infiltrated with extraction buffer [400 mM sucrose, 10 mM 2-(*N*-morpholine)-ethanesulphonic acid (MES), pH 5.3, 10 mM NaCl, 5 mM $MgCl_2$, 5 mM EDTA, 0.1% Triton X-100, 1 mM phenylmethylsulphonyl fluoride (PMSF), 0.1 mM DTT and 1x complete protease inhibitor] and ground in 9 ml of the same buffer. After passage through a 100-μm filter, the lysate was layered on top of a discontinuous gradient consisting of successive 4-ml layers of iodixanol 15% and 45% in the extraction buffer. The discontinuous gradient was centrifuged at 1500 ***g*** for 15 min at 4°C. the cytoplasmic fraction was obtained from the top of the 15% iodixanol layer, and the nuclei fraction was obtained from the 15/45% iodixanol interface. The pure nuclei were washed three times with the extraction buffer. A 10-mg portion of whole-cell extract and the corresponding equivalent cytoplasmic and nuclear fractions were used for Western blot analysis.

GUS-reporter construction and enzyme activity assay

The genomic fragment of *AtNAP1;4* was PCR amplified using primers N4-Pro-5′ and N4-Pro-3′ (see Table S2), and was then cloned into the *Hin*dIII–*Sma*I restriction sites of vector pBI101, resulting in pAtNAP1;4::AtNAP1;4-GUS. This construct contains a 619-bp upstream section of the predicted translational start site, and all exons and introns of *AtNAP1;4*, and is fused in frame with the reporter *GUS* at the last exon. The construct was introduced into Arabidopsis plants by *Agrobacterium*-mediated transformation. A histochemical GUS enzyme activity assay was performed as described by Yu *et al.* (2003). The essential results were reproducibly obtained from more than 10 plants for each transgenic line.

RT-PCR

Total RNA was prepared using the TRIzol kit according to the manufacturer's instructions (Invitrogen). Semiquantitative RT-PCR

was performed using Improm-II reverse transcriptase (Promega, http://www.promega.com) and quantitative RT-PCR with the kit from Takara (http://www.takara-bio.com). The gene-specific primers used in the PCR analysis are presented in Table S2.

Microarray

Six-day-old homozygous *m123-1*, *m123-2* and wild-type *Col* (control) seedlings were harvested, and total RNA was prepared using the TRIzol kit (Invitrogen). The microarray analyses were performed by using Affymetrix gene chips at Shanghai Huaguan Biochip (http://www.hgbiochip.com/english.html). Data analysis was performed using GENESPRING 5 software (Silicon Genetics, now part of Agilent, http://www.agilent.com). The expression profiles, each in duplicate, of *m123-1* and *m123-2* plants were compared with those of wild-type *Col* plants (*m123-1* versus *Col* and *m123-2* versus *Col*). Genes of *m123-1* and *m123-2* mutant plants exhibiting the same increase or decrease in expression level in each replicate were considered as upregulated or downregulated, respectively. In addition, a threshold of twofold or greater change was used for producing the final lists of upregulated and downregulated genes in *m123-1* and *m123-2*.

UV treatment and *in vitro* DNA repair assay

To evaluate the plant response to UV, 8-day-old *in vitro* germinated plants were irradiated with a dose of 3750 J m^{-2} of UV-C (254 nm) using a Minerallight-Lamp (UVP, http://www.uvp.com) three times every 24 h. Plants were immediately returned to the growth chamber after each exposure. The phenotype was observed 13 days after the last UV treatment. For analysis of gene expression in response to UV treatment, 6-day-old seedlings were irradiated three times with 500 J m^{-2} UV-C, and then incubated for recovery in a growth chamber for 2 h before RNA isolation.

The *in vitro* DNA repair assay was performed according to the method described by Li *et al.* (2002). The linearized pGEX plasmid was treated by UV-C (450 J m^{-2}) using the Stratalinker (Stratagene, http://www.stratagene.com) to increase the DNA damage. We used 25 μg of plant protein extracts per time point mixed with 300 ng of UV-C-treated pGEX, together with 300 ng of linearized pBSK plasmid, which was not pre-treated by UV-C. Incorporation of DIG-labeled 2′-deoxyuridine-5′-triphosphate (dUTP) in the plasmids was detected as previously described by Li *et al.* (2002).

ChIP analysis

About 2 g of 6-day-old seedlings were used for ChIP analysis, which was performed as described by Zhao *et al.* (2005). The gene-specific primers used in the ChIP analysis are presented in Table S2.

ACKNOWLEDGEMENTS

We thank Jean Molinier for help with the plasmid DNA repair assay, Léon Otten for help with the nuclei preparation experiments and for a critical reading of the manuscript. The work in the AD's laboratory was supported in part by grants from the National Natural Science Foundation of China (30570933, 30628004 and 30800630), the Chinese Ministry of Science and Technology (2009CB825601) and the Ministry of Agriculture (2008ZX08009). ZL and JG are supported by fellowships for foreign students from the French Ministère de l'Education Nationale, de l'Enseignement Supérieur et de la Recherche. YF is supported by PICS exchange grants, and research in W-HS's laboratory is supported by the Centre National de la Recherche Scientifique (CNRS).

SUPPORTING INFORMATION

Additional Supporting Information may be found in the online version of this article:

Figure S1. Alignment of amino acid sequences of Arabidopsis NAP1-family proteins.

Figure S2. A schematic representation of procedures for obtaining the double and triple *Atnap1* mutants.

Table S1. List of differentially expressed genes found in the triple *Atnap1* mutants *m123-1* and *m123-2*.

Table S2. List of primers used in this study.

Please note: Wiley-Blackwell are not responsible for the content or functionality of any supporting materials supplied by the authors. Any queries (other than missing material) should be directed to the corresponding author for the article.

REFERENCES

Altman, R. and Kellogg, D. (1997) Control of mitotic events by Nap1 and the Gin4 kinase. *J. Cell Biol.* **138**, 119–130.

Angelov, D., Bondarenko, V.A., Almagro, S. *et al.* (2006) Nucleolin is a histone chaperone with FACT-like activity and assists remodeling of nucleosomes. *Embo J* **25**, 1669–1679.

Azimzadeh, J., Nacry, P., Christodoulidou, A., Drevensek, S., Camilleri, C., Amiour, N., Parcy, F., Pastuglia, M. and Bouchez, D. (2008) Arabidopsis TONNEAU1 proteins are essential for preprophase band formation and interact with centrin. *Plant Cell*, **20**, 2146–2159.

Belotserkovskaya, R., Oh, S., Bondarenko, V.A., Orphanides, G., Studitsky, V.M. and Reinberg, D. (2003) FACT facilitates transcription-dependent nucleosome alteration. *Science*, **301**, 1090–1093.

Clark, J., Alvarez, D.F., Alexeyev, M., King, J.A., Huang, L., Yoder, M.C. and Stevens, T. (2008) Regulatory role for nucleosome assembly protein-1 in the proliferative and vasculogenic phenotype of pulmonary endothelium. *Am. J. Physiol. Lung Cell. Mol. Physiol.* **294**, L431–L439.

Costa, R.M., Morgante, P.G., Berra, C.M., Nakabashi, M., Bruneau, D., Bouchez, D., Sweder, K.S., Van Sluys, M.A. and Menck, C.F. (2001) The participation of AtXPB1, the XPB/RAD25 homologue gene from *Arabidopsis thaliana*, in DNA repair and plant development. *Plant J.* **28**, 385–395.

De Koning, L., Corpet, A., Haber, J.E. and Almouzni, G. (2007) Histone chaperones: an escort network regulating histone traffic. *Nat. Struct. Mol. Biol.* **14**, 997–1007.

Dinant, C., Houtsmuller, A.B. and Vermeulen, W. (2008) Chromatin structure and DNA damage repair. *Epigenetics Chromatin*, **1**, 9.

Dong, A., Zhu, Y., Yu, Y., Cao, K., Sun, C. and Shen, W.H. (2003) Regulation of biosynthesis and intracellular localization of rice and tobacco homologues of nucleosome assembly protein 1. *Planta*, **216**, 561–570.

Dong, A., Liu, Z., Zhu, Y., Yu, F., Li, Z., Cao, K. and Shen, W.H. (2005) Interacting proteins and differences in nuclear transport reveal specific functions for the NAP1 family proteins in plants. *Plant Physiol.* **138**, 1446–1456.

Duroux, M., Houben, A., Ruzicka, K., Friml, J. and Grasser, K.D. (2004) The chromatin remodelling complex FACT associates with actively transcribed regions of the Arabidopsis genome. *Plant J.* **40**, 660–671.

Galichet, A. and Gruissem, W. (2006) Developmentally controlled farnesylation modulates AtNAP1;1 function in cell proliferation and cell expansion during Arabidopsis leaf development. *Plant Physiol.* **142**, 1412–1426.

Garcia, V., Bruchet, H., Camescasse, D., Granier, F., Bouchez, D. and Tissier, A. (2003) AtATM is essential for meiosis and the somatic response to DNA damage in plants. *Plant Cell*, **15**, 119–132.

Kojima, H., Suzuki, T., Kato, T. *et al.* (2007) Sugar-inducible expression of the nucleolin-1 gene of *Arabidopsis thaliana* and its role in ribosome synthesis, growth and development. *Plant J.* **49**, 1053–1063.

Kunz, B.A., Anderson, H.J., Osmond, M.J. and Vonarx, E.J. (2005) Components of nucleotide excision repair and DNA damage tolerance in *Arabidopsis thaliana*. *Environ. Mol. Mutagen.* **45**, 115–127.

Lankenau, S., Barnickel, T., Marhold, J., Lyko, F., Mechler, B.M. and Lankenau, D.H. (2003) Knockout targeting of the Drosophila nap1 gene and examination of DNA repair tracts in the recombination products. *Genetics*, **163**, 611–623.

Li, A., Schuermann, D., Gallego, F., Kovalchuk, I. and Tinland, B. (2002) Repair of damaged DNA by Arabidopsis cell extract. *Plant Cell*, **14**, 263–273.

Li, W., Chen, C., Markmann-Mulisch, U., Timofejeva, L., Schmelzer, E., Ma, H. and Reiss, B. (2004) The Arabidopsis AtRAD51 gene is dispensable for vegetative development but required for meiosis. *Proc. Natl Acad. Sci. USA*, **101**, 10596–10601.

Liang, L., Flury, S., Kalck, V., Hohn, B. and Molinier, J. (2006) CENTRIN2 interacts with the Arabidopsis homolog of the human XPC protein (AtRAD4) and contributes to efficient synthesis-dependent repair of bulky DNA lesions. *Plant Mol. Biol.* **61**, 345–356.

Luger, K., Mader, A.W., Richmond, R.K., Sargent, D.F. and Richmond, T.J. (1997) Crystal structure of the nucleosome core particle at 2.8 A resolution. *Nature*, **389**, 251–260.

Molinier, J., Ramos, C., Fritsch, O. and Hohn, B. (2004) CENTRIN2 modulates homologous recombination and nucleotide excision repair in Arabidopsis. *Plant Cell*, **16**, 1633–1643.

Morgante, P.G., Berra, C.M., Nakabashi, M., Costa, R.M., Menck, C.F. and Van Sluys, M.A. (2005) Functional XPB/RAD25 redundancy in Arabidopsis genome: characterization of AtXPB2 and expression analysis. *Gene*, **344**, 93–103.

Ohkuni, K., Shirahige, K. and Kikuchi, A. (2003) Genome-wide expression analysis of NAP1 in *Saccharomyces cerevisiae*. *Biochem. Biophys. Res. Commun.* **306**, 5–9.

Osakabe, K., Abe, K., Yoshioka, T., Osakabe, Y., Todoriki, S., Ichikawa, H., Hohn, B. and Toki, S. (2006) Isolation and characterization of the RAD54 gene from *Arabidopsis thaliana*. *Plant J.* **48**, 827–842.

Park, Y.J. and Luger, K. (2006a) Structure and function of nucleosome assembly proteins. *Biochem. Cell Biol.* **84**, 549–558.

Park, Y.J. and Luger, K. (2006b) The structure of nucleosome assembly protein 1. *Proc. Natl Acad. Sci. USA* **103**, 1248–1253.

Petricka, J.J. and Nelson, T.M. (2007) Arabidopsis nucleolin affects plant development and patterning. *Plant Physiol.* **144**, 173–186.

Pontvianne, F., Matia, I., Douet, J., Tourmente, S., Medina, F.J., Echeverria, M. and Saez-Vasquez, J. (2007) Characterization of AtNUC-L1 reveals a central role of nucleolin in nucleolus organization and silencing of AtNUC-L2 gene in Arabidopsis. *Mol. Biol. Cell*, **18**, 369–379.

Rogner, U.C., Spyropoulos, D.D., Le Novere, N., Changeux, J.P. and Avner, P. (2000) Control of neurulation by the nucleosome assembly protein-1-like 2. *Nat. Genet.* **25**, 431–435.

Sancar, A. (1996) DNA excision repair. *Annu. Rev. Biochem.* **65**, 43–81.

Xu, L., Xu, Y., Dong, A., Sun, Y., Pi, L., Xu, Y. and Huang, H. (2003) Novel as1 and as2 defects in leaf adaxial-abaxial polarity reveal the requirement for ASYMMETRIC LEAVES1 and 2 and ERECTA functions in specifying leaf adaxial identity. *Development*, **130**, 4097–4107.

Yoon, H.W., Kim, M.C., Lee, S.Y., Hwang, I., Bahk, J.D., Hong, J.C., Ishimi, Y. and Cho, M.J. (1995) Molecular cloning and functional characterization of a cDNA encoding nucleosome assembly protein 1 (NAP-1) from soybean. *Mol. Gen. Genet.* **249**, 465–473.

Yu, Y., Steinmetz, A., Meyer, D., Brown, S. and Shen, W.H. (2003) The tobacco A-type cyclin, Nicta;CYCA3;2, at the nexus of cell division and differentiation. *Plant Cell*, **15**, 2763–2777.

Zhao, Z., Yu, Y., Meyer, D., Wu, C. and Shen, W.H. (2005) Prevention of early flowering by expression of FLOWERING LOCUS C requires methylation of histone H3 K36. *Nat. Cell Biol.* **7**, 1256–1260.

Zhu, Y., Dong, A., Meyer, D., Pichon, O., Renou, J.P., Cao, K. and Shen, W.H. (2006) Arabidopsis NRP1 and NRP2 encode histone chaperones and are required for maintaining postembryonic root growth. *Plant Cell*, **18**, 2879–2892.

